Textures and Microstructures, 1988, Vols. 8 & 9, pp. 97–114
Reprints available directly from the publisher
Photocopying permitted by license only

Printed in the United Kingdom

ODF Calculation by Series Expansion from Incompletely Measured Pole Figures Using the Positivity Condition Part II—All Crystal Symmetries

M. DAHMS,† H. J. BUNGE

Institut für Metallkunde und Metallphysik der TU Clausthal; Großer Bruch 23; D-3392 Clausthal-Zellerfeld. † Now: GKSS-Forschungszentrum; Max-Planck-Straße; D-2054 Geesthacht

(Received September 3, 1987)

Dedicated to the memory of Professor Günter Wassermann

The calculation of orientation distribution functions (ODF) from incomplete pole figures of any crystal symmetry can be carried out by an iterative procedure taking into account the positivity condition for all pole figures. During the iterative procedure the pole figures are normalized and the pole figure inversion leads to stable results, i.e. the coefficients for higher degrees of series expansion keep small.

KEY WORDS: ODF calculation, iterative method, incomplete pole figures, positivity condition, normalization factor, ε-brass, tin.

INTRODUCTION

In a previous paper (Dahms and Bunge (1987)), a new method for the calculation of an orientation distribution function (ODF) from incompletely measured pole figures has been presented. This method uses an iterative procedure in which the positivity condition

$$P_{hkl}(\alpha\beta) \geq 0 \qquad (1)$$

for any pole figure desired is taken into account. Because the normalization of the incomplete pole figures was carried out by cubic extrapolation (Dahms and Bunge (1986)), this procedure can only be used for pole figures from samples possessing cubic crystal symmetry. It is the aim of this paper to generalize the method, such that it can be used for any crystal symmetry.

MATHEMATICAL FUNDAMENTALS

(see also Dahms and Bunge (1987))

In the harmonic method, the coefficients $F_l^\nu(hkl)$ of a pole figure are related to the coefficients $C_l^{\mu\nu}$ of the ODF by

$$F_l^\nu(hkl) = \frac{4\pi}{2l+1} \sum_{\mu=1}^{M(l)} C_l^{\mu\nu} \dot{k}_l^\mu(hkl) \tag{2}$$

where $\dot{k}_l^\mu(hkl)$ are spherical surface harmonics satisfying crystal symmetry.

The pole density values $P_{hkl}(\alpha\beta)$ of the corresponding pole figures can be calculated from

$$P_{hkl}(\alpha\beta) = \sum_{l=0}^{L} \sum_{\mu=1}^{N(l)} F_l^\nu(hkl) \dot{k}_l^\nu(\alpha\beta) \tag{3}$$

where $\dot{k}_l^\nu(\alpha\beta)$ are spherical surface harmonics satisfying sample symmetry.

In the case of completely measured pole figures, $F_l^\nu(hkl)$ can be calculated from

$$F_l^\nu(hkl) = \int_{\alpha=0}^{\pi} \int_{\beta=0}^{2\pi} P_{hkl}(\alpha\beta) \dot{k}_l^{*\nu}(\alpha\beta) \sin\alpha \, d\alpha \, d\beta \tag{4}$$

where * denotes the complex conjugate quantity.

The normalized pole density $P_{hkl}(\alpha\beta)$ cannot be measured directly. It must be determined from the measured intensity $I_{hkl}(\alpha\beta)$ using the relation

$$P_{hkl}(\alpha\beta) = N_{hkl} \cdot I_{hkl}(\alpha\beta) \tag{5}$$

where N_{hkl} can be determined from the normalization condition $F_0^1 = \sqrt{4\pi}$.

Thus, for completely measured pole figures, Eq. (2) is an overdetermined system of linear equations because normally more than $M(l)$ pole figures are measured. This problem may be solved using a least squares method

$$\sum_i w_i \left[F_l^\nu(hkl_i) - \frac{4\pi}{2l+1} \sum_{\mu=1}^{M(l)} C_l^{\mu\nu} k_l^\mu(hkl_i) \right]^2 = \min \tag{6}$$

with w_i as a weight factor.

The so determined $C_l^{\mu\nu}$ do not necessarily fulfill the positivity condition, Eq. (1), but normally this doesn't introduce serious errors, if pole figures with low indices are chosen for the ODF analysis.

In the case of incomplete pole figures, the pole figure coefficients $F_l^\nu(hkl)$ cannot be determined directly from the pole figure values. They are defined by a twofold integral of which one part is known and the other is unknown:

$$F_l^\nu(hkl)/N_{hkl} = 2 \cdot \int_{\alpha=0}^{\alpha_{\max}} \int_{\beta=0}^{2\pi} I_{hkl}(\alpha\beta) \dot{k}_l^\nu(\alpha\beta) \sin\alpha \, d\alpha \, d\beta + 2 \cdot \int_{\alpha=\alpha_{\max}}^{\pi/2} \int_{\beta=0}^{2\pi} I_{hkl}(\alpha\beta) \dot{k}_l^\nu(\alpha\beta) \sin\alpha \, d\alpha \, d\beta \tag{7}$$

The I_{hkl} in the unknown part of the pole figures can be approximated by any expression. Here, a simple quadratic β-independent polynomial is suggested:

$$I_{hkl}(\alpha\beta) = A + B\alpha + C\alpha^2 = W_{hkl}(\alpha) \tag{8}$$

the coefficients of which are obtained from boundary conditoins at $\alpha = \alpha_{\max}$ and $\alpha = \pi/2$. Details of this procedure were given in an earlier paper (Dahms and Bunge (1986)). Using this approximation, the second part of Eq. (7) is zero for any $\nu \neq 1$.

Thus, the pole figures can be normalized approximatively and first order $F_l^\nu(hkl)$ can be calculated. Using Eq. (6), first order $C_l^{\mu\nu}$ can be calculated, and from these $F_l^\nu(hkl)$ and $P_{hkl}(\alpha\beta)$ can be recalculated. Because of Eq. (1), all negative pole figure values can be set to zero.

Now, a second order estimation of the N_{hkl} can be obtained using

the integral version of Eq. (5):

$$\int_{\alpha=0}^{\alpha_{\max}}\int_{\beta=0}^{2\pi} P_{hkl}(\alpha\beta)\sin\alpha\, d\alpha\, d\beta = N_{hkl}\int_{\alpha=0}^{\alpha_{\max}}\int_{\beta=0}^{2\pi} I_{hkl}(\alpha\beta)\sin\alpha\, d\alpha\, d\beta \tag{9}$$

This method is similar to Van Houtte's (1980) iterative method, who did, however, not include the positivity condition.

A second order estimation of the unknown part of Eq. (7) is now possible, thus leading to a second order estimation of the $F_l^{\nu}(hkl)$. In this way a loop is defined, which can be run through as often as desired. There is no risk of divergency, because no negative values are allowed according to Eq. (1). The flow diagram for the procedure described here can be seen in Figure 1.

Also in this iterative procedure, it is possible to introduce additional not measured pole figures after the first loop. They can be treated in the same way as the measured pole figures, but no iterative normalization is necessary. This may be useful, if the number of measured pole figures is too small compared with the desired degree of series expansion L given by the value $M(L)$ in Eq. (2). In this case, Eq. (2) is underdetermined and thus cannot be solved without additional conditions. In the case that $M(L)$ equals the number of pole figures, all errors which may occur in the pole figures are projected into the $C_l^{\mu\nu}$ via the error-containing $F_l^{\nu}(hkl)$. Additional pole figures bound to the positivity condition may generally lead to overdetermined systems of linear equations, which may be solved by the least-squares method Eq. (6).

RESULTS

In order to test the suggested methods, one synthetic and two real textures were used.

The synthetic texture was a hexagonal $(0001)\langle 10\bar{1}0\rangle$ texture with a spread of 12.5°. Figure 2 shows the corresponding ODF ($L = 22$, $\varphi_2 = \text{const.}$). Theoretical pole figures were calculated as described earlier (Dahms and Bunge (1986)) in steps of $\Delta\alpha = 5°$ and $\Delta\beta = 3.6°$ up to $\alpha_{\max} = 70°$ in the approximation $L = 22$ with c/a = 1.5873 (Titanium). (0001), $(10\bar{1}0)$, $(11\bar{2}0)$, $(10\bar{1}2)$ and $(11\bar{2}2)$ pole figures were obtained (see Figure 3). Because of the specific

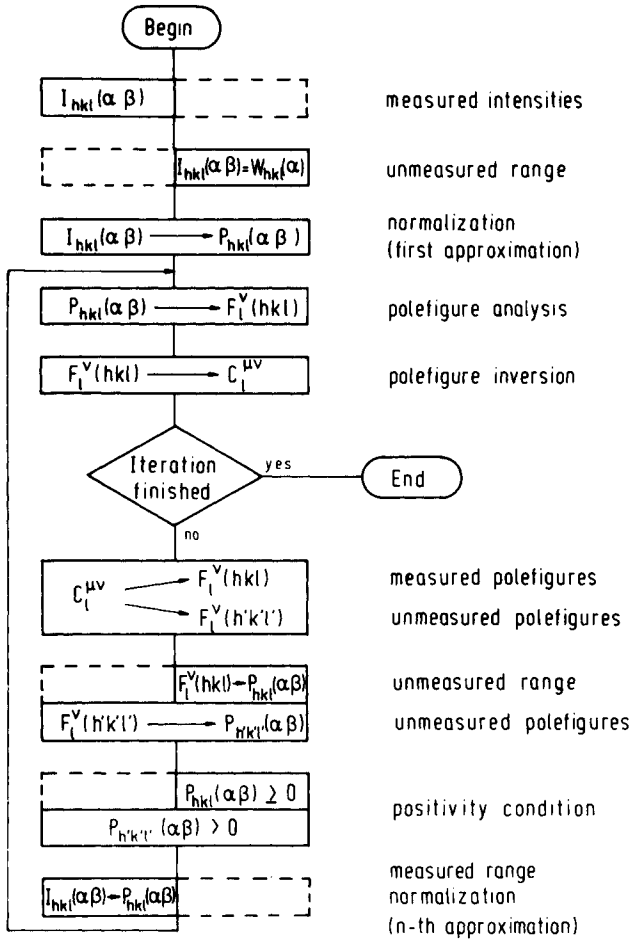

Figure 1 Flow diagram of the iterative procedure.

features of this texture, they possessed also hexagonal sample symmetry, but they were treated in the general orthorhombic symmetry. This texture was chosen, because in this case, the normalization of some of the incomplete pole figures is extremely difficult. For all pole figures of the type (*hki*0), nearly all the expected pole density is contained in the unmeasured range. Hence, this texture presents a rather strong test of the proposed method.

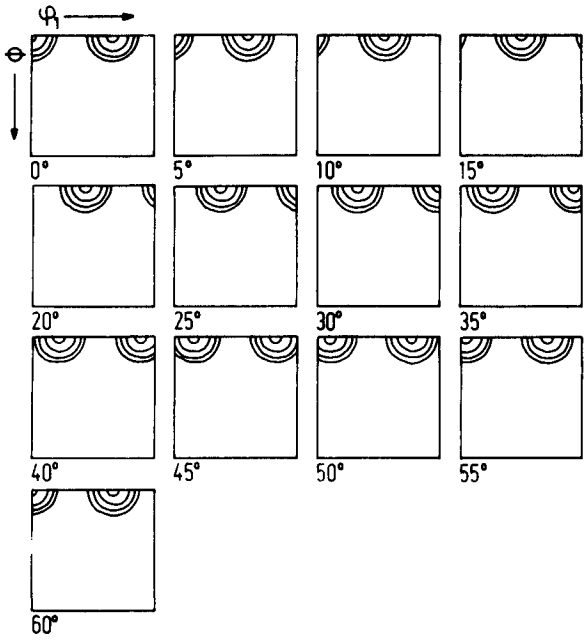

Figure 2 Theoretical ODF of a hexagonal $(0001)\langle 10\bar{1}0\rangle$ texture ($\varphi_2 = \text{const.}$, $L = 22$, contour levels 12, 25, 50, 100 × random).

The first real texture was the texture of the alloy ZnCu15 (ε-brass), which was extruded at 480°C from 75 mm ϕ to $7 \times 35\ \text{mm}^2$. Here the same pole figures as above and the $(10\bar{1}3)$ pole figure were measured with the same steps to $\alpha_{\max} = 70°$ using Cu(Kα) radiation, they are shown in Figure 4. In the micrograph of the longitudinal section (Figure 5), a banded recrystallized structure can be seen.

The second texture was the texture of a tin sheet, which was rolled 95.75% at room temperature. The (200), (101), (220), (211), (301) and (112) pole figures were measured in the same way as the brass pole figures but using the oblique section method as presented by Welch (1980). Here the effect of an additional not measured pole figure to the ODF analysis will be shown. The pole figures after rotation to the standard projection and symmetrization can be seen in Figure 6. In the micrograph of the longitudinal section (Figure 7) also a recrystallized structure is found.

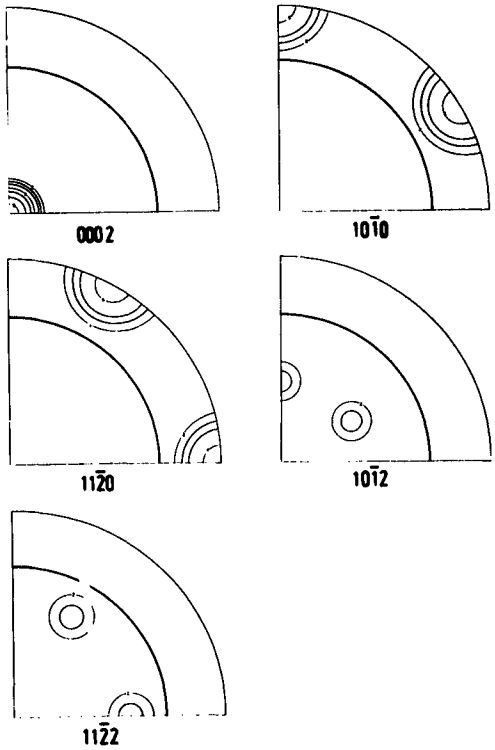

Figure 3 Pole figures of the texture of Figure 2 with marked limiting tilt angle $\alpha_{max} = 70°$ for incomplete pole figures (c/a = 1.5873, contour levels 2, 3, 4, 6, 8, 12, 16, 24 × random).

Theoretical Texture

The five incomplete pole figures of Figure 3 were roughly normalized using quadratic extrapolation Eq. (8). The so obtained normalization factors were used as starting values for the following iterative procedure. During the iteration, the normalization factors changed continuously, which can be seen in Figure 8 for the case of the (10$\bar{1}$0) pole figure. The normalization factor converges to unity but very slowly. Table 1 shows the normalization factors obtained by the quadratic extrapolation and after 21st loop.

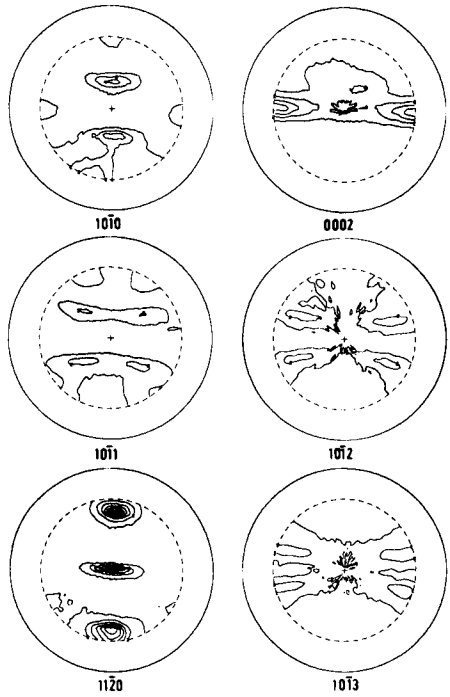

Figure 4 Incomplete pole figures of ε-brass extruded at 480°C from 75 mm ϕ to 7×35 mm^2 (contour levels $1, 2, \ldots, 7 \times$ random).

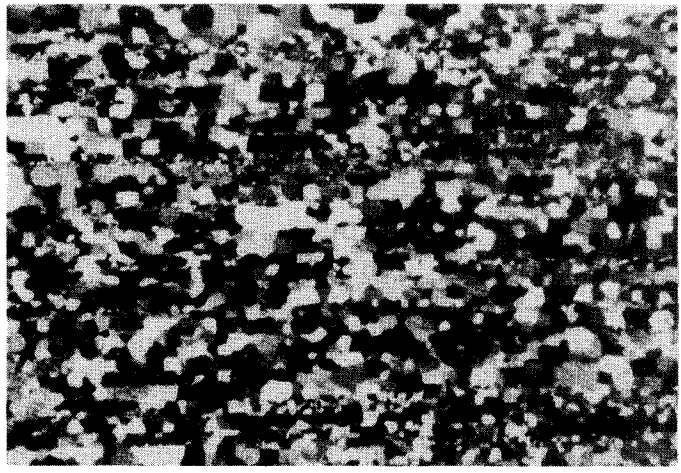

Figure 5 Longitudinal section of the extruded ε-brass.

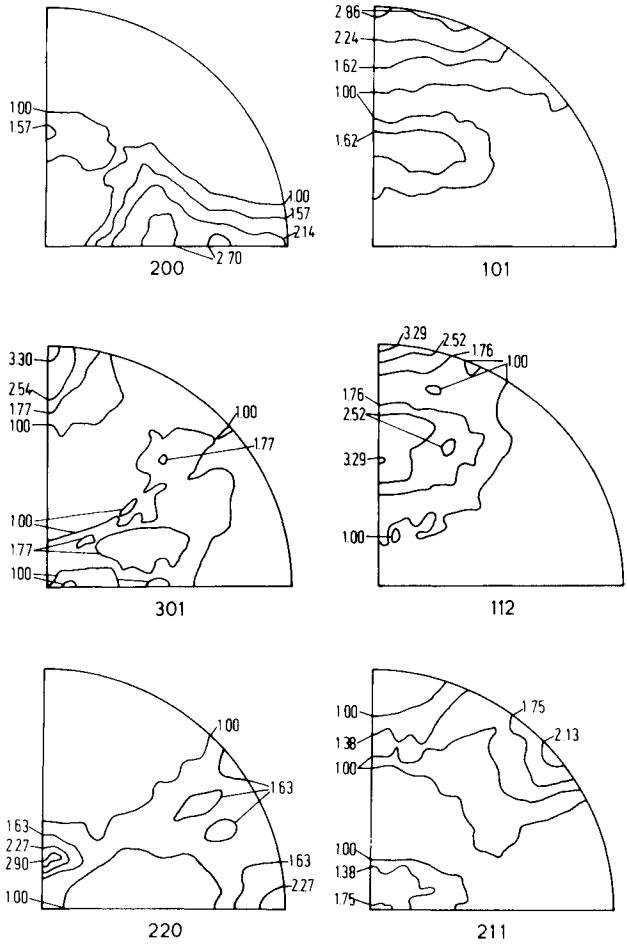

Figure 6 Symmetrized pole figures of 93.75% rolled tin, recrystallized at room temperature (contour levels in multiples of the random intensity).

It can be seen that the errors of the normalization factors of two pole figures (about 20%) are rather high. Nevertheless it must be taken into account that in these two cases the P_{hkl} in the "measured" ranges are extremely low such that the absolute error is low, too.

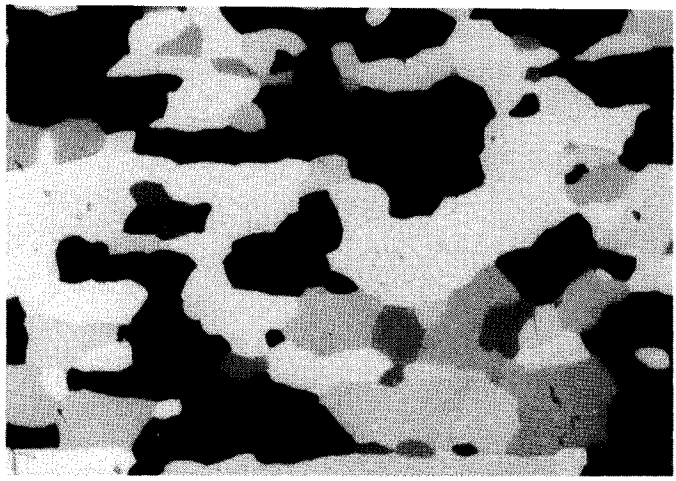

Figure 7 Longitudinal section of the rolled tin sheet.

Within the same loops as the normalization factors, also the $C_l^{\mu\nu}$ were calculated up to $L = 22$. In Table 2, all non-zero coefficients are given compared to the theoretical values. (The $C_l^{\mu\nu}$ are independent of the index ν in this case.)

It is seen that the C_l^{11} i.e. the fibre texture components are well

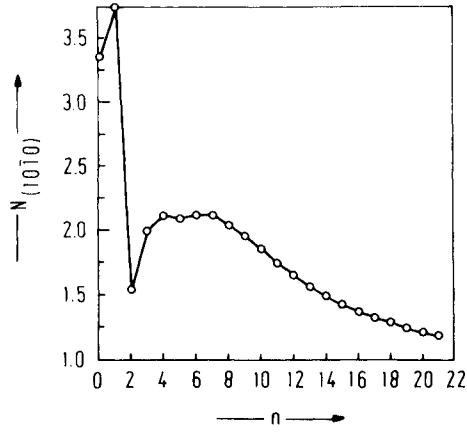

Figure 8 Change of the normalization factor of the (10$\bar{1}$0) pole figure of the (0001)⟨10$\bar{1}$0⟩-texture during the iterative procedure.

Table 1 Normalization factors of incomplete pole figures of a $(0001)\langle 10\bar{1}0\rangle$ texture with $\omega_0 = 12.5°$ before and after the iterative procedure (The ideal value is 1)

hkil	N_{hkil} Initial	21st loop
(0001)	0.999	1.003
$(10\bar{1}0)$	3.345	1.201
$(11\bar{2}0)$	3.345	1.171
$(10\bar{1}2)$	1.039	1.002
$(11\bar{2}2)$	1.147	1.003

represented after the 21st loop, although the normalization factors show considerable errors, while the errors increase with increasing ν. Nevertheless, they correspond with the theoretical one, even in this extremely unfavourable case, within a reasonable order of magnitude and the so obtained solution is stable. In Table 3 the maximum values of the ODF and the texture index (Sturcken and Croach (1963)) of the theoretical and the iteratively calculated ODFs are shown.

Iterative texture analysis from incomplete pole figures leads, as it is seen, to a somewhat smoothed ODF. This can also be seen in Figure 9, where two sections of the ODF (even l) are shown. No additional artefacts or oscillations are introduced by this method.

Table 2 Theoretical and interatively calculated $C_l^{\mu\nu}$-values from incomplete pole figures

l	Theor. all μ and ν	21st loop μ ν 1 1	μ ν 2 4	μ ν 3 7	μ ν 4 10
2	4.656	4.667			
4	7.097	7.115			
6	7.895	7.897	7.643		
8	7.230	7.240	7.055		
10	5.687	5.675	5.564		
12	3.921	3.927	3.915	2.486	
14	2.395	2.374	2.609	1.707	
16	1.305	1.321	1.562	1.063	
18	0.637	0.624	0.614	0.694	0.358
20	0.280	0.299	0.362	0.439	0.078
22	0.111	0.096	0.255	0.417	0.079

Table 3 Texture indices J and maximum values of the ODF (f_{max}) of a $(0001)\langle 10\bar{1}0\rangle$ texture calculated from theoretical coefficients and from incomplete pole figures (even l)

	J	f_{max}
Theor.	33.9	81.3
Incom.	31.5	78.2

Texture of extruded ε-brass

The coefficients $C_l^{\mu\nu}$ were calculated iteratively up to $L = 22$. In Table 4, the normlization factors obtained by quadadratic extrapolation and after the 21st loop are shown.

It is clearly seen that the change of the normalization factors during the iterative procedure is less then 10%. It can be concluded that quadratic extrapolation is a good method to estimate the normalization of an incomplete pole figure.

The $C_l^{\mu\nu}$ for odd l-values were calculated using the zero range method as presented by Lee *et al.* (1986). The zero range was defined in the recalculated pole figures. A pole figure point with a pole density $<0.33 \times$ random was assumed to belong to the "physical" zero range according to Welch *et al.* (1987). The mean

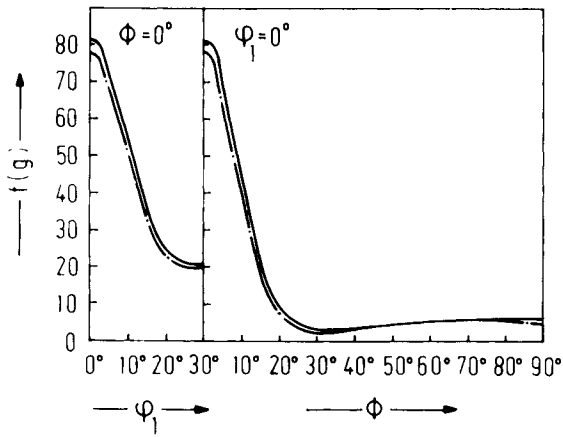

Figure 9 Section of the ODF of the $(0001)\langle 10\bar{1}0\rangle$ texture (even l, $\varphi_2 = 0°$, (——) theoretical ODF, (—·—) ODF from incomplete pole figures).

Table 4 Change of the normalization factors from the quadratic extrapolation (N_a) to the final value (N_e)

hkil	N_a	N_e
$(10\bar{1}0)$	0.4448	0.3861
(0002)	0.3951	0.3731
$(10\bar{1}1)$	0.1076	0.1002
$(10\bar{1}2)$	0.8795	0.8482
$(11\bar{2}0)$	0.8787	0.8163
$(10\bar{1}3)$	0.8726	0.8584

absolute $C_l^{\mu\nu}$ vs. l are shown in Figure 10. Additionally, the errors for even l are marked. It can be seen that the coefficients for odd l are in the range of the errors for the even l. This is due to the fact that there is a strong fibre component in the texture.

The complete ODF is shown in Figure 11. The main texture component is a $(11\bar{2}0)\langle 10\bar{1}0\rangle$ texture at (0°, 90°, 0°) which is superposed by a $\langle 10\bar{1}0\rangle$ fibre texture with its axis parallel to the extrusion direction. This can also be seen in Figure 12, where a section of the ODF at $\varphi_1 = \varphi_2 = 0°$ is shown. The superposition of these two types of textures is due to the extrusion process. An ideal fibre texture would be expected in the case of a circular profile.

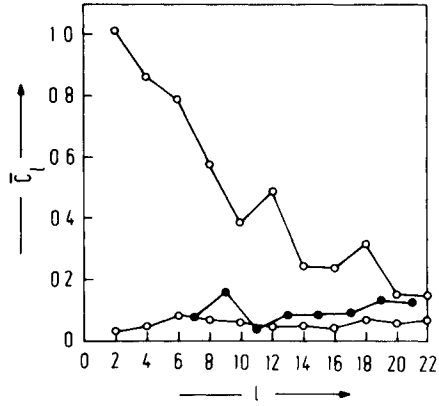

Figure 10 Mean absolute values of the coefficients $C_l^{\mu\nu}$ vs. degree of series expansion of extruded ε-brass: (○) even l (lower curve errors); (●) odd l.

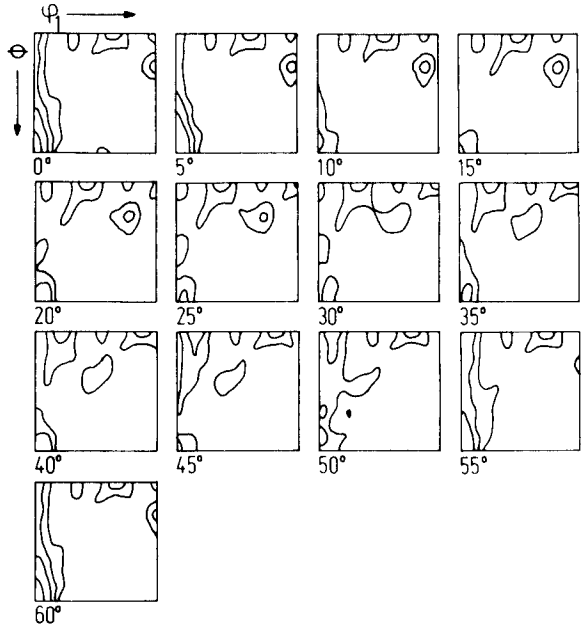

Figure 11 Complete ODF of extruded ε-brass ($\varphi_2 = \text{const.}$, $L = 22$, contour levels $3, 6, 12, 24 \times$ random).

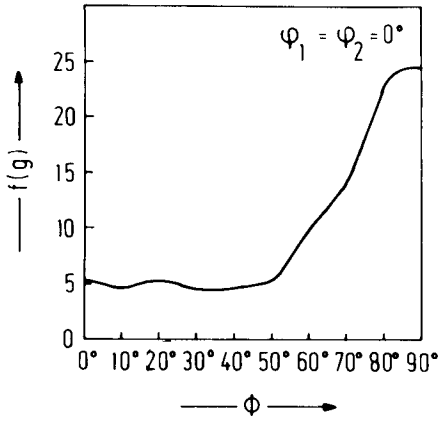

Figure 12 Section through the ODF of Figure 11.

Texture of rolled tin

In this case, complete experimental pole figures were available, but their number was too low in order to solve Eq. (6) up to a satisfactory degree which was chosen as $L = 20$. Because of the tetragonal symmetry, it is $M(20) = 6$. In order to level out experimental errors in the pole figures it is desirable, however to use at least seven pole figures. Hence, the (001) pole figure, which cannot be measured experimentally was introduced in the way described above. Since the (001) pole figure has the lowest multiplicity of all pole figures in tin, it has large ranges of low or zero intensity in which the positivity condition adds information to the mathematical procedure by which the coefficients $C_l^{\mu\nu}$ are determined. The mean absolute values of the resulting C-coefficients for the first and the 19th iteration steps are shown in Figure 13. The improvement of the solution obtained by introducing the (001) pole figure is to be seen in Figure 14 showing that the negative values were considerably reduced.

Again, using the zero-range method, $C_l^{\mu\nu}$ for odd l were calculated up to $L = 21$ starting from the "even" ODF without and with additional (001) pole figure. With these coefficients complete ODFs were calculated, which are shown in Figure 15a,b. It is

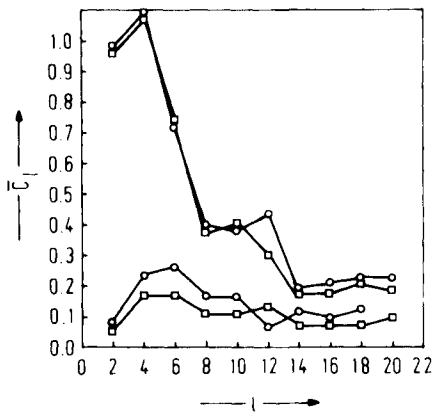

Figure 13 Mean absolute values of the coefficients $C_l^{\mu\nu}$ vs. degree of series expansion of rolled tin: (○) first estimate; (□) after the 19th loop (lower curves errors).

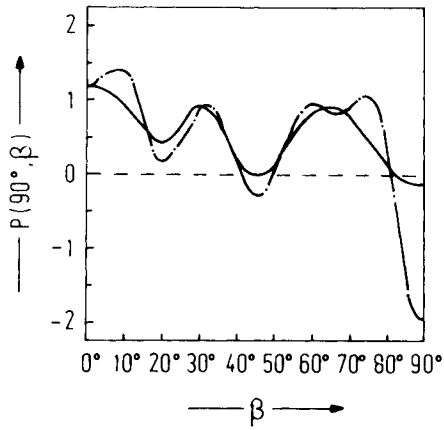

Figure 14 Circle $\alpha = 90°$ of the calculated (001) pole figure: (—·—) first estimate (——) after the 19th loop.

clearly seen that some of the spread orientations have disappeared in the latter case.

The accuracy of the ODF can be estimated by the resulting negative values, either by the maximum negative value (which is the minimum value f_{min} of the ODF) or by the integral over the negative region S_-. These values are given in Table 5 along with the maximum value and the texture index. The latter ones show a slight decrease of the sharpness of the obtained ODF whereas the former ones show a considerable decrease of the errors obtained by the introduction of the (001) pole figure in the iterative process.

CONCLUSIONS

The iterative method described here including iterative normalization and taking into account the positivity condition of all pole figures allows the calculation of the ODF from incompletely measured pole figures of all crystal symmetries. For lower crystal symmetries, the positivity condition may be used to introduce additional pole figures, which stabilize the coefficients of high order. By that way, higher degrees of series expansion are possible and false peaks introduced by series truncation are reduced. This

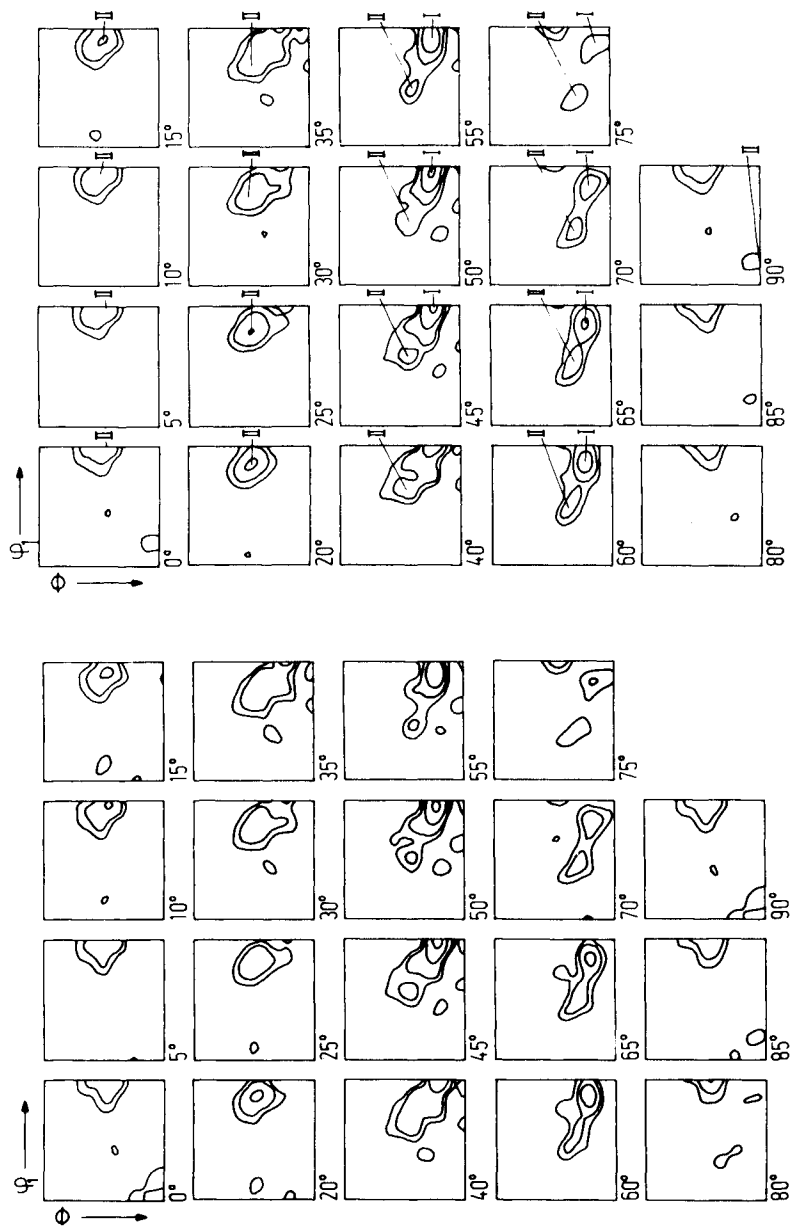

Figure 15 Complete ODFs of cold rolled tin (φ_2 = const., $L = 20$): a) first estimate b) after the 19th loop.

Table 5 Texture index J (even l), maximum (f_{max}) and minimum value (f_{min}) and weighted sum of negative intensities S_- of the complete ODF of a rolled tin sheet

	J	f_{max}	f_{min}	S_-
Without (001)	3.95	20.6	−3.7	623
With (001)	3.63	19.6	−1.7	383

method can easily be implemented at any standard system of pole figure inversion using complete pole figures.

References

Bunge, H. J. (1982). *Texture Analysis in Materials Science* Butterworth London.
Dahms, M. & Bunge, H. J. (1986). *Textures and Microstructures* **6,** 167–179.
Dahms, M. & Bunge, H. J. (1987). *Textures and Microstructures* **7,** 171–185.
Van Houtte, P. (1980). *Mat. Sci. Eng.* **43,** 7–11.
Lee, H. P., Bunge, H. J. & Esling, C. (1986). *Textures and Microstructures* **6,** 289–313.
Sturcken, E. F. & Croach, J. W. (1963). *TMS-AIME* **227,** 934–940.
Welch, P. I. (1980). *Texture* **4,** 99–111.
Welch, P. I., Dahms, M. and Bunge, H. J. (1987). In: Theoretical Methods of Texture Analysis, Ed. H. J. Bunge, DGM Informationsgesellschaft Verlag 63–77.